Supporting Information

In vitro cytotoxicity and adaptive stress responses to selected haloacetic acid and halobenzoquinone water disinfection by-products

Erik Procházka[*†], Beate I. Escher[†,‡,§], Michael J. Plewa[‖,⊥], Frederic D.L. Leusch[†]

[†]Griffith University, Smart Water Research Centre, Australian Rivers Institute, School of Environment, Gold Coast, Queensland, Australia

[‡]UFZ - Helmholtz Centre for Environmental Research, Cell Toxicology, Leipzig, Germany

[§]Eberhard Karls University Tübingen, Center for Applied Geosciences, Environmental Toxicology, Tübingen, Germany

[‖]University of Illinois at Urbana-Champaign, Department of Crop Sciences, Urbana, IL, U.S.A.

[⊥]University of Illinois at Urbana-Champaign, Safe Global Water Institute and the Science and Technology Center of Advanced Materials for the Purification of Water with Systems, Urbana, IL, U.S.A.

[*]Smart Water Research Centre (G51),

Griffith University, Gold Coast Campus,

Parklands Drive, Southport,

Queensland 4222, Australia.

Email: e.prochazka@griffith.edu.au

Phone: +61 7 5552 7814

Captions of Tables and Figures

Table S1 *In vitro* impact on cell viability of selected DBPs in Caco-2 cell line using neutral red uptake (NRU), 4h exposure.

Figure S1 Changes in cytotoxicity following immediate dosing of HBQs versus dosing following 1h delay with HBQs dissolved in assay medium, presented as % Negative Control ±SE; A) 2,6-dichloro-*p*-benzoquinone (DCBQ), B) 2,6-dibromo-*p*-benzoquinone (DBBQ).

Figure S2 Comparison of changes in cytotoxicity immediate dosing of HBQs versus dosing following 1h delay with HBQs dissolved in assay medium (F12), presented as IC_{50} (μM); lower value indicates higher cytotoxicity.

Figure S3 Caco-2 acute (4h) cytotoxicity (MTS) concentration-response curves for: A) HAAs, and B) HBQs; presented as % Negative Control.

Figure S4 Pathway specific activity of the selected 5 DBPs; Oxidative stress-responsive ARE-*bla*, and DNA damage-responsive p53RE-*bla*; Assay activity presented as $1/EC_{IR1.5}$ (μM) ±SE.

Figure S5 CHO chronic (72h) cytotoxicity dose-response curves for the two HBQs, presented as % Negative Control ±SE.

Figure S6 Cytotoxicity of HBQs in 2 cell lines, Caco-2 (4h) and CHO (72h), presented as % Negative Control ±SE; A) 2,6-dichloro-*p*-benzoquinone (DCBQ), B) 2,6-dibromo-*p*-benzoquinone (DBBQ).

Figure S7 Caco-2 (NRU) cytotoxicity concentration-response curves of selected HAAs, presented as % Negative Control ±SE; A) Chloroacetic acid (CAA), B) Bromoacetic acid (BAA), C) Iodoacetic acid (IAA).

Figure S8 Caco-2 (NRU) cytotoxicity concentration-response curves of selected HBQs, presented as % Negative Control ±SE; A) 2,6-dichloro-*p*-benzoquinone (DCBQ), B) 2,6-dibromo-*p*-benzoquinone (DBBQ).

HBQ reactivity with assay media and its impact on cytotoxicity

Caco-2 cells did not show difference in cytotoxic response to HBQs dosed immediately or with a delay of 1h (Figure S1), however we found a pronounced difference in CHO cell cytotoxic response depending on the addition of the HBQ to the cells, either immediately (direct) or with >20 minute incubation in the assay media (F12) (Figure S2). The medium showed a rapid change in colour and when this altered medium was added to cells the toxic response was lower than when we added the HBQs to the microplate immediately with cells present.

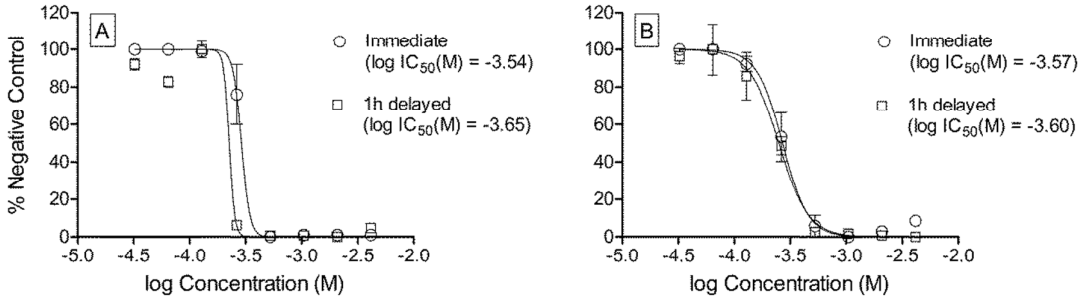

Figure S1 Changes in cytotoxicity following immediate dosing of HBQs versus dosing following 1h delay with HBQs dissolved in assay medium, presented as % Negative Control ±SE; A) 2,6-dichloro-*p*-benzoquinone (DCBQ), B) 2,6-dibromo-*p*-benzoquinone (DBBQ).

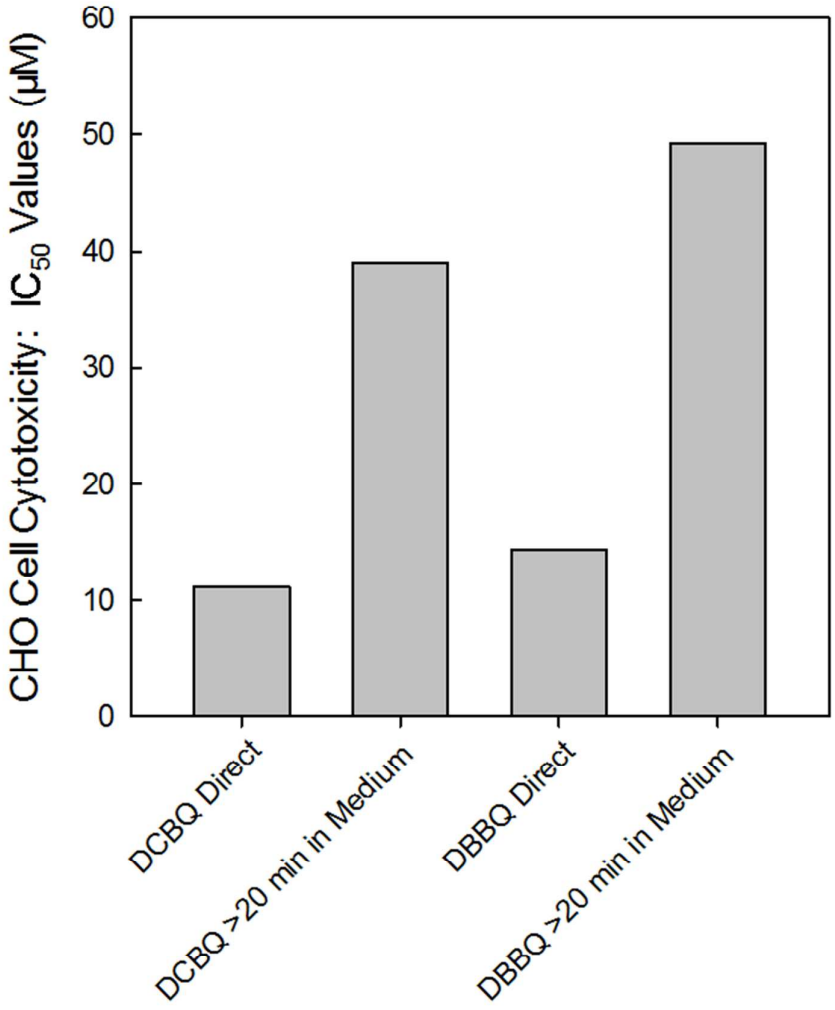

Figure S2 Comparison of changes in cytotoxicity immediate dosing of HBQs versus dosing following 1h delay with HBQs dissolved in assay medium (F12), presented as IC_{50} (µM); lower value indicates higher cytotoxicity.

Caco-2 acute cytotoxicity assay procedure

The Caco-2 cytotoxicity assay was performed as described in Leusch et al.[1] with minor modifications. To summarize briefly, we prepared each of the tested DBPs as a concentrated stock in methanol (MeOH) up to a concentration of 1 M or, in case of HBQs, to a limit of solubility (~0.25 M). We then followed the standard procedure described in Leusch et al.[1] seeding the plates at density of 2×10^4 per well using Scepter cell counter (Millipore) in 96-well microtiter plates (Greiner Bio-one Cellstar; Cat# 655-180); using PBS (pH 7.4, Invitrogen), 0.12% (w/v) trypsin/EDTA (Invitrogen) solution and growth medium (DMEM/F12 with Phenol Red, Invitrogen). On Day 2 of the assay we removed the growth medium from each test well using a vacuum aspirator and washed each well twice with 150µL of warm (37°C) PBS (pH 7.4), then added 50µL of assay medium (DMEM/F12 without Phenol Red) into each test well. We then added serially diluted DBPs into the test wells to a total volume of 100µL per well, leaving a no-treatment control (i.e., negative control). After 4h of incubation at 37°C and 5% CO_2, we again washed the cells with PBS (2×), and followed the manufacturer's instructions for Promega CellTiter 96® Aqueous One Solution Cell Proliferation Assay Kit[2], measuring absorbance at 490 nm using a Fluostar Omega (BMG Labtech, Germany) plate reader.

For each DBP we generated an *in vitro* Caco-2 cytotoxicity concentration-response curve (Figure S1) combining the data from all the individual runs (minimum of two individual runs on two separate days). We first converted the absolute absorbance values to % mean absorbance of untreated cell control wells (i.e., % negative control) by first subtracting the mean background absorbance from the absolute absorbance value of each test well, then dividing the resulting value by the mean absorbance of the negative control, and finally multiplying by 100. We then normalized the data in GraphPad Prism® 5.0 for Windows

using the program's "Normalize" function to standardize slight fluctuations between each run and plotted the % negative control values against the log concentration (M) and calculated median inhibition concentrations (IC_{50}) for each of the DBPs using the "log(inhibitor) *vs* response (four parameter)" model in GraphPad Prism® 5.0 for Windows, while anchoring the bottom constraint to 0% and the top to 100%.

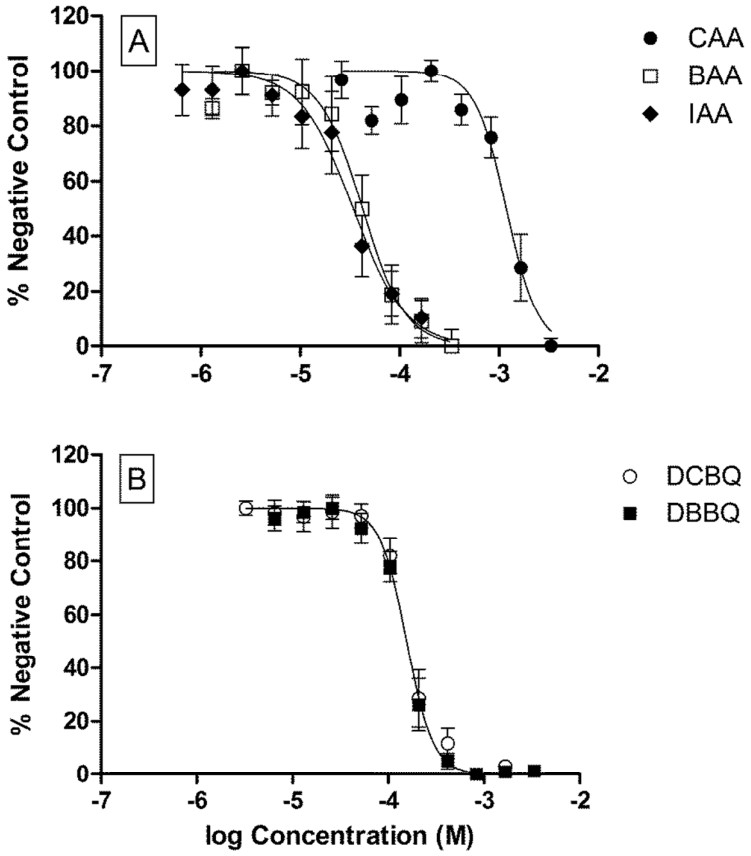

Figure S3 Caco-2 acute (4h) cytotoxicity (MTS) concentration-response curves for: A) HAAs, and B) HBQs; presented as % Negative Control.

ARE-*bla* and p53RE-*bla* assay procedures

We used two CellSensor™ (Invitrogen) cell-based assays utilizing the GeneBLAzer™ technology, ARE-*bla* and p53RE-*bla*, to evaluate oxidative stress and DNA damage response, respectively. The exposure times for the assays were as per standard manufacturer's protocol, 15h and 16h for the ARE-*bla* and p53RE-*bla*, respectively.[3,4]

The protocols were modified to a small degree: fluorescence emission was read at 520nm instead of 530nm due to technical limitations of the microplate reader used (FLUOstar Omega, BMG Labtech; Mornington, Vic, Australia); half of the amount of 'Solution A' and 'Solution B' were added into the final incubation step; and a two-fold and 12-fold reduction of the amount of 'Solution D' was added into the final incubation step for the p53RE-*bla* and ARE-*bla*, respectively.

In order to determine the pathway-specific *in vitro* activity (Figure S2) in ARE-*bla* and p53-*bla* assays, we calculated the effect concentrations corresponding to 1.5× the induction ratio ($EC_{IR1.5}$) using a method described in detail by Escher et al.[5]

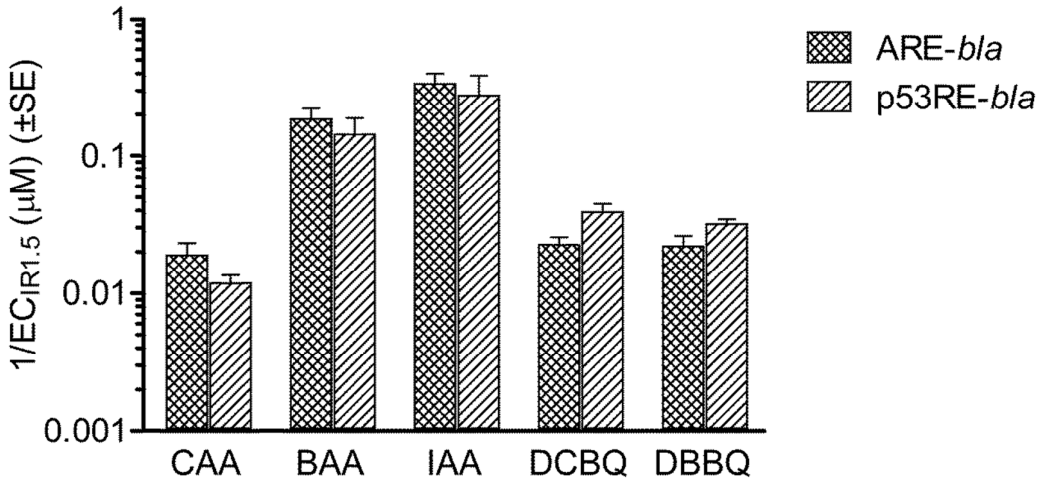

Figure S4 Pathway specific activity of the selected 5 DBPs; Oxidative stress-responsive ARE-*bla*, and DNA damage-responsive p53RE-*bla*; Assay activity presented as $1/EC_{IR1.5}$ (μM) ±SE.

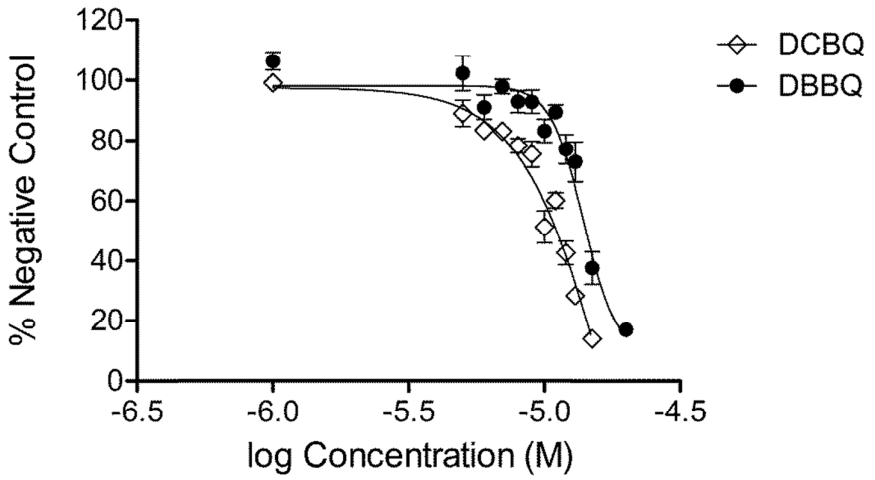

Figure S5 CHO chronic (72h) cytotoxicity dose-response curves for the two HBQs, presented as % Negative Control ±SE.

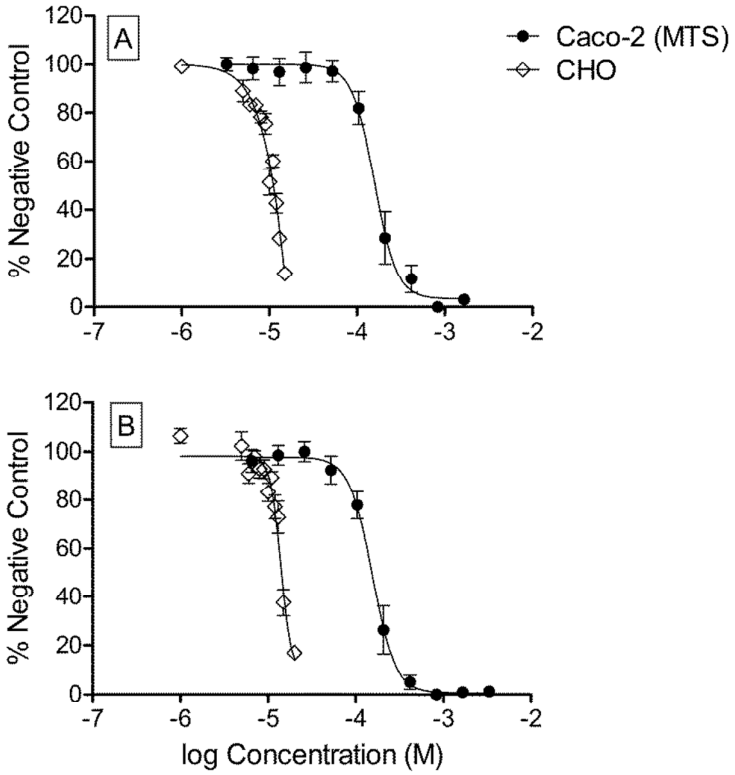

Figure S6 Cytotoxicity of HBQs in 2 cell lines, Caco-2 (4h) and CHO (72h), presented as % Negative Control ±SE; A) 2,6-dichloro-*p*-benzoquinone (DCBQ), B) 2,6-dibromo-*p*-benzoquinone (DBBQ).

Table S2 *In vitro* impact on cell viability of selected DBPs in Caco-2 cell line using neutral red uptake (NRU), 4h exposure.

Compound/ Endpoint	**log IC_{50}/M[#] ± SE**	**IC_{50}[#] (μM)**
CAA	-2.91 ± 0.02	1240
BAA	-4.18 ± 0.03	65
IAA	-4.56 ± 0.03	27
DCBQ	-3.64 ± 0.02	228
DBBQ	-3.47 ± 0.03	339

[#]mean value

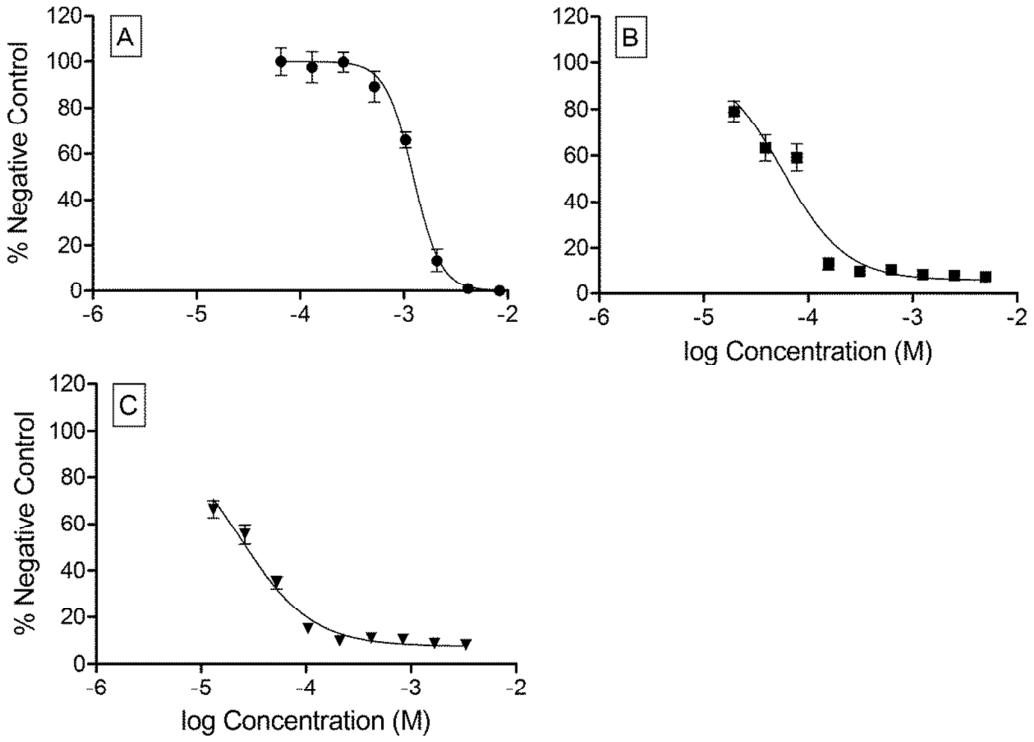

Figure S7 Caco-2 (NRU) cytotoxicity concentration-response curves of selected HAAs, presented as % Negative Control ±SE; A) Chloroacetic acid (CAA), B) Bromoacetic acid (BAA), C) Iodoacetic acid (IAA).

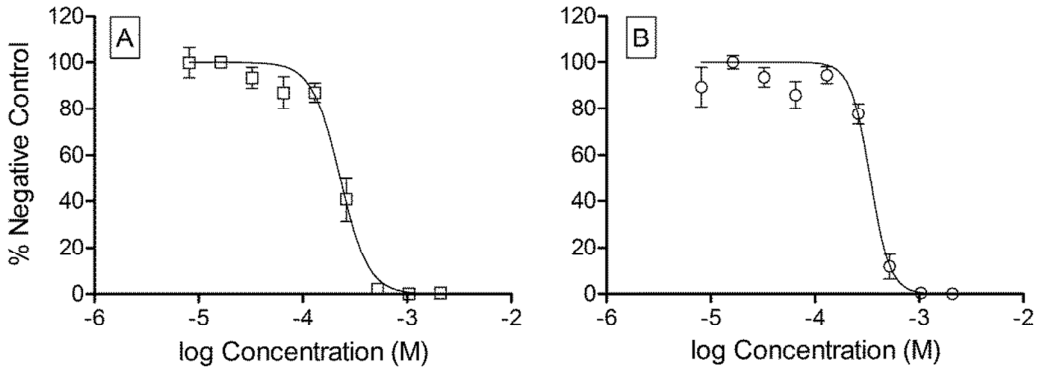

Figure S8 Caco-2 (NRU) cytotoxicity concentration-response curves of selected HBQs, presented as % Negative Control ±SE; A) 2,6-dichloro-*p*-benzoquinone (DCBQ), B) 2,6-dibromo-*p*-benzoquinone (DBBQ).

References

(1) Leusch, F. D. L., Khan, S. J., Laingam, S., Prochazka, E., Froscio, S., Trinh, T., Chapman, H. F., and Humpage, A. (2014) Assessment of the application of bioanalytical tools as surrogate measure of chemical contaminants in recycled water. *Water Res. 49*, 300-315.

(2) Promega. (2012) Technical Bulletin - CellTiter 96 AQueous One Solution Cell Proliferation Assay (Instructions for Use of Products G3580, G3581 and G3582), Promega Corporation, Madison, WI, USA. https://www.promega.com/~/media/files/resources/protocols/technical%20bulletins/0/celltiter%2096%20aqueous%20one%20solution%20cell%20proliferation%20assay%20system%20protocol.pdf (accessed June 30, 2015).

(3) Invitrogen. (2010) CellSensor™ p53RE-bla HCT-116 Cell-based Assay Protocol, K1202, In *Invitrogen Cell-based Assay Protocols*, http://tools.lifetechnologies.com/content/sfs/manuals/cellsensor_p53HCT116_man.pdf (accessed June 30, 2015).

(4) Invitrogen. (2006) CellSensor™ ARE-bla Hep G2 Cell-based Assay Protocol, K1208, In *Invitrogen Cell-based Assay Protocols*, http://tools.lifetechnologies.com/content/sfs/manuals/cellsensor_AREblaHepG2_man.pdf (accessed June 30, 2015).

(5) Escher, B. I., Dutt, M., Maylin, E., Tang, J. Y. M., Toze, S., Wolf, C. R., and Lang, M. (2012) Water quality assessment using the AREc32 reporter gene assay indicative of the oxidative stress response pathway. *J. Environ. Monit. 14*, 2877-2885.